The ISME Journal (2013) 7, 1725–1737

www.nature.com/ismej

ORIGINAL ARTICLE

Oxygen-dependent niche formation of a pyrite-dependent acidophilic consortium built by archaea and bacteria

Sibylle Ziegler[1,2], Kerstin Dolch[2], Katharina Geiger[2], Susanne Krause[2], Maximilian Asskamp[1], Karin Eusterhues[3], Michael Kriews[4], Dorothee Wilhelms-Dick[5], Joerg Goettlicher[6], Juraj Majzlan[3] and Johannes Gescher[2]

[1]*Department of Microbiology, Albert-Ludwigs University, Freiburg, Germany;* [2]*Department of Applied Biology, Karlsruhe Institute of Technology, Karlsruhe, Germany;* [3]*Department of Mineralogy, Friedrich Schiller University, Jena, Germany;* [4]*Department of Geosciences/Glaciology, Alfred Wegener Institute for Polar and Marine Research, Bremerhaven, Germany;* [5]*Department of Geoscience, University of Bremen, Bremen, Germany and* [6]*Institute for Synchrotron Radiation, Karlsruhe Institute of Technology, Karlsruhe, Germany*

Biofilms can provide a number of different ecological niches for microorganisms. Here, a multispecies biofilm was studied in which pyrite-oxidizing microbes are the primary producers. Its stability allowed not only detailed fluorescence *in situ* hybridization (FISH)-based characterization of the microbial population in different areas of the biofilm but also to integrate these results with oxygen and pH microsensor measurements conducted before. The O_2 concentration declined rapidly from the outside to the inside of the biofilm. Hence, part of the population lives under microoxic or anoxic conditions. *Leptospirillum ferrooxidans* strains dominate the microbial population but are only located in the oxic periphery of the snottite structure. Interestingly, archaea were identified only in the anoxic parts of the biofilm. The archaeal community consists mainly of so far uncultured *Thermoplasmatales* as well as novel ARMAN (Archaeal Richmond Mine Acidophilic Nanoorganism) species. Inductively coupled plasma analysis and X-ray absorption near edge structure spectra provide further insight in the biofilm characteristics but revealed no other major factors than oxygen affecting the distribution of bacteria and archaea. In addition to catalyzed reporter deposition FISH and oxygen microsensor measurements, microautoradiographic FISH was used to identify areas in which active CO_2 fixation takes place. Leptospirilla as well as acidithiobacilli were identified as primary producers. Fixation of gaseous CO_2 seems to proceed only in the outer rim of the snottite. Archaea inhabiting the snottite core do not seem to contribute to the primary production. This work gives insight in the ecological niches of acidophilic microorganisms and their role in a consortium. The data provided the basis for the enrichment of uncultured archaea.

The ISME Journal (2013) **7,** 1725–1737; doi:10.1038/ismej.2013.64; published online 25 April 2013
Subject Category: microbial population and community ecology
Keywords: acid mine drainage; *Leptospririllum*; *Acidithionbacillus*; ecological niche; ARMAN; thermoplasmatales

Introduction

Acidification occurs often in mining areas where due to mining activities sulfide ores are exposed to an oxic environment. Interestingly, ferric iron and not oxygen is the most influential oxidant for pyrite (FeS_2), the most abundant sulfide mineral. The abiotic reoxidation of the produced ferrous iron is a rather slow process under low pH conditions. This process is enormously accelerated by the activity of acidophilic aerobic chemolithotrophic iron-oxidizing microorganisms (Singer and Stumm, 1970). The end products of pyrite dissolution are sulfuric acid and ferric iron. Hence, acidic waters containing high concentrations of metals are formed. This process, called acid mine drainage, is a major threat for the environment in mining areas (Nordstrom, 2000; Johnson and Hallberg, 2005).

A number of microbial species have adapted to acid mine drainage conditions. These are characterized by a high concentration in metalloids and sulfuric acid as well as the availability of only inorganic carbon and oxygen. *Leptospirillum* as well as *Acidithiobacillus* strains are well-known members of the microbial population in mining areas and fulfill the above mentioned chemolithotrophic

Correspondence: J Gescher, Department of Applied Biology, Karlsruhe Institute of Technology, Fritz Haber Weg 2, Karlsruhe 76131, Germany.
E-mail: johannes.gescher@kit.edu
Received 31 October 2012; revised 1 March 2013; accepted 11 March 2013; published online 25 April 2013

requirements. The element cycling carried out by these pioneer organisms gives rise to other ecological niches, which can be colonized by further groups of microorganisms. Typically, biofilms are the macroscopic manifestations of such coexisting populations. In acidic habitats, these biofilms are not only found often in the form of acid streamers but also as snottites, which are morphologically similar to stalactites but have a rather gel-like character. Examples of such acidic biofilms can be found in a number of field sites (Bond *et al.*, 2000; Hallberg *et al.*, 2006; García-Moyano *et al.*, 2007; Kimura *et al.*, 2011). Inside those biofilms, possible niches are defined, for instance, by the availability of inorganic and organic carbon as well as terminal electron acceptors. The characterization of these niches is important to understand the role of microorganisms in the biofilms and potentially enables isolation of so far uncultivated microorganisms.

Organisms that were found in acid mine drainage biofilms are primarily iron- and/or sulfur-oxidizing bacteria and archaea like *Leptospirillum* spp., *Acidithiobacillus* spp., *Acidimicrobium* spp., *Ferrimicrobium* spp. and *Ferroplasma* spp., as well as iron- or sulfur-reducing organisms like *Acidithiobacillus* spp., *Acidiphilium* spp., *Acidimicrobium* spp., *Ferrimicrobium* spp., *Ferroplasma* spp. or *Thermoplasma* spp. (Bond *et al.*, 2000; Dopson *et al.*, 2004; García-Moyano *et al.*, 2007; Ziegler *et al.*, 2009; Kimura *et al.*, 2011). Interestingly, some of the members of the *Thermoplasmatales* found by culture-independent methods in acidic mining areas are—judging from the 16S rDNA sequences—quite distinct from the isolated representatives (Rowe *et al.*, 2007; Gonzalez-Toril *et al.*, 2011). Hence, it is possible to taxonomically classify them, but it has to be questioned whether these organisms have the same capabilities as the known isolates. Furthermore, novel archaea, called ARMAN (Archaeal Richmond Mine Acidophilic Nanoorganism) were recently discovered by shotgun sequencing of specimens that were sampled at the Iron Mountain Superfund Site in California. They belong to deeply branching lineages that were not found previously owing to mismatches of the hitherto believed universal archaea primer sets (Baker *et al.*, 2006). Using metagenomic and proteomic data, it was assumed that these novel archaea are aerobic chemoheterotrophs.

This study focuses on acidic biofilms that were found in an abandoned pyrite mine. Only three levels of this mine are accessible. Previously, biofilms from the adit level of the mine were studied (Ziegler *et al.*, 2009). Ziegler *et al.* (2009) described the bacterial community and mineralogy of this snottites. *Leptospirillum ferrooxidans* and *Ferrovum* sp. species dominated the microbial population, whereas archaea could not be detected. The aim of this study was to evaluate the different ecological niches that are occupied and formed by the microorganisms in biofilms of the first level, 29 m deeper than the adit level. Therefore, oxygen concentrations and pH values were recorded using microsensor measurement systems. These experiments were accompanied by cryo-laser ablation inductively coupled plasma mass spectrometry (LA-ICP-MS), ICP optical emission spectrometry (OES) and X-ray absorption near edge structure (XANES) analysis to specify the chemical composition of the potential niches in a greater detail. The microbial composition of the biofilm was evaluated using catalyzed reporter deposition fluorescence *in situ* hybridization (CARD FISH). Furthermore, primary production in the biofilm was assessed using microautoradiography (MAR). Results of this study give insights into physiological capabilities of acidophilic microorganisms under environmental conditions. They additionally suggest an anaerobic lifestyle for members of the ARMAN, which were so far believed to grow aerobically. In order to proof the assumptions regarding the lifestyle of Archaea and ARMAN in the biofilm, enrichment experiments using anoxic culture techniques were started.

Materials and methods

Field site

All samples used in this work were exclusively snottite biofilms and collected from or studied at the first level of the abandoned pyrite mine *Drei Kronen und Ehrt* in the Harz Mountains in Germany. The mine has only three accessible levels. Lower parts of the mine were flooded. The adit level is located 428 m above sea level and was studied in the work from Ziegler *et al.* (2009). The first level is 399 m above sea level. Differences in those two levels are in pH and iron concentrations as stated in the results of this work.

Metagenomic analysis

DNA was isolated from 1 g snottite material from the first level according to the protocol from Lo *et al.* (2007) with the following modifications: frozen biofilm material was homogenized under liquid nitrogen using a mortar. Cells were then washed in 15 ml phosphate-buffered saline pH 2.1. After centrifugation, the pellet was resuspended in 5 ml 50 mM Tris pH 7.5/50 mM EDTA pH 8.0. In all, 150 μl lysozyme solution (100 mg ml^{-1}) was added and incubation took place at 37 °C for 1.5 h. Also, 1 ml STEP buffer containing 20 mg ml^{-1} Proteinase K was added and incubated over night at 50 °C. The phenol/chloroform/isoamyl DNA extraction method was used as described before (Lo *et al.*, 2007). The shotgun metagenomic sequencing was done by a 454 GS Titanium (Roche, Branford, CT, USA). It produced the totality of 754 643 *reads*, with an average length of 366 bp. The contig assembly generated 10 573 continuous sequences with an average length of 1571 bp and a GC (guanine-cytosine) content of

52.2%. Reads were analyzed using MetaSAMS (Zakrzewski *et al.*, 2012). Detected 16S rRNA gene sequences were further analyzed using the classification tool from the Ribosomal Database Project web interface (RDP Naive Bayesian rRNA Classifier Version 2.5, May 2012, confidence value of 80%) (Cole *et al.*, 2009). Using this binary identification procedure, 692 reads with classifiable 16S rDNA information were gained.

Restriction fragment length polymorphism analysis
DNA was isolated from a frozen, homogenized biofilm using the innuSPEED Soil DNA kit (Analytic Jena, Jena, Germany) according to the manufacturer's instructions. Three different primer pairs were used for archaeal 16S rDNA amplification. General archaea primer (Supplementary Table S2, primers 1 + 2) and ARMAN primers (Supplementary Table S2, primers 3 + 4) were used. For further identification of archaea, the forward primer was deduced from the ARCH915 probe and applied together with an universal reverse primer (Supplementary Table S2, primers 6 + 5).

Sequence analysis
16S rDNA sequence analysis and similarity comparison were performed using the Ribosomal Database Project (http://rdp.cme.msu.edu) and the BLAST program of the National Center for Biotechnology Information (http://www.ncbi.nlm.nih.gov). The phylogenetic tree was calculated using the neighbor-joining method. For further information see Supplementary 'Materials and Methods'.

Microsensor measurements
Oxygen concentrations and pH values were determined directly in the hanging snottites in the mine. The biofilm was moved slightly by the microsensor but stayed stable. The profiles were measured using a microprofiling setup from Pyro Science (Aachen, Germany).

^{14}C labeling
Snottites were labeled with $^{14}CO_2$ directly in the mine; 3 MBq (81 μCi) of $NaH^{14}CO_3$ were used per snottite. A 1-L incubation chamber was mounted and sealed around the biofilms. The radioactive bicarbonate was dissolved in 100 μM Tris pH 10.5. Bicarbonate was converted to CO_2 gas by addition of 10 N H_2SO_4 through an injection spot from the outside. The incubation time was 22 h. A pasteurized snottite was used as a negative control. It was treated as described above and incubated for 23 h.

Fixation and embedding of the samples
Snottites from the microsensor measurements and the $^{14}CO_2$ labeling were fixed directly in 4% formaldehyde in *Leptospirillum*-medium (132 mg l^{-1} $(NH_4)_2SO_4$, 53 mg l^{-1} $MgCl_2 \cdot 6H_2O$, 27 mg l^{-1} KH_2PO_4 and 147 mg l^{-1} $CaCl_2 \cdot 2H_2O$). The pH of the medium was adjusted to 2.5 with 10 N H_2SO_4. Fixation was carried out for 6–8 h at 4 °C. Thereafter, biofilms were washed twice in the medium and three times in 1 × phosphate-buffered saline in each case for 10 min (Zielinski *et al.*, 2009). Afterwards, samples were subdivided in five pieces, embedded into Steedman's wax and cut with a microtome (Leica Microsystems, Wetzlar, Germany) in 5–6 μm slices and transferred to Polysine slides (Thermo Scientific, Braunschweig, Germany) (Steedman, 1957).

CARD FISH
Embedded samples were first dewaxed and rehydrated. Hybridization and amplification was done as described by Pernthaler *et al.* (2004) with minor modifications as described in the Supplementary section SI Materials and Methods.

MAR FISH
The above described CARD FISH procedure was also used for the detection of CO_2 fixation. The MAR was performed in the dark room according to Rogers (1979) and Okabe *et al.* (2004). Hypercoat LM1 (GE Healthcare, Freiburg, Germany) coated slides were incubated for 4 months.

Determination of elemental compositions
Cryo-laser ablation ICP-MS. LA-ICP-MS was performed by coupling the Elan6000 (Perkin Elmer/Sciex, Rodgau, Germany) to the Indi-40 Spectra Physics LA system (basis wavelength 1064 nm). Within this work, the quadrupled wavelength of 266 nm was used. As LA chamber, the cryo chamber described by Kriews *et al.* (2001; 2004) and Reinhardt *et al.* (2001) was used with minor modifications that are listed together with scanning procedure in the Supplementary section SI Materials and Methods.

ICP-OES and ICP-MS. Sample preparation was conducted with whole flashfrozen snottite material from which the oxic parts (≈1 mm) were dissected off using a razor blade. The samples from oxic and anoxic parts were centrifuged, thereafter filtered and subjected to ICP-MS measurement. The analyses were conducted in triplicate with ICP-OES Spectroflame (Spectro, Kleve, Germany) or ICP-MS X-Series II (ThermoFisher Scientific, Schwerte, Germany) instruments.

Iron and sulfate quantification. Iron und sulfate quantification was conducted from whole snottite biofilms from the first level of the pyrite mine. The biofilm was centrifuged at 10 000 *g* for 10 min, and the supernatant was analyzed. Ferrous and total iron were quantified as described before

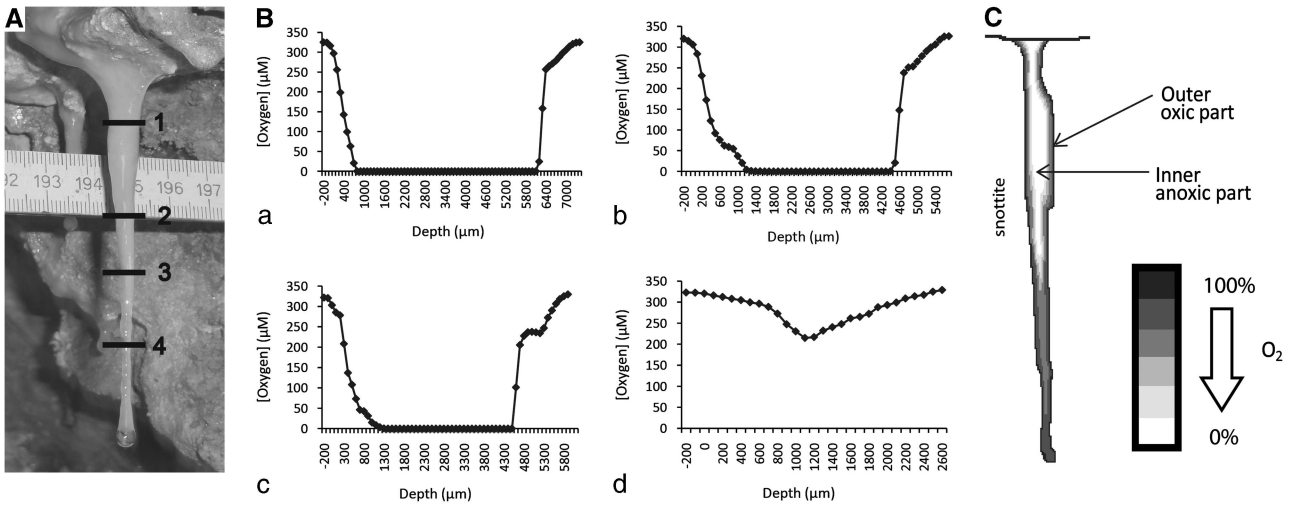

Figure 1 Oxygen profile measurements in the snottite. (**A**) Location of oxygen profiles across a snottite biofilm, taken at distances of 1, 3, 4.5 and 6 cm from the ceiling. (**B**) Oxygen profiles. (a) The profile taken closest to the rock surface shows the fastest oxygen decrease: at a depth of 700 µm, oxygen was no longer detectable. (b and c) show anoxic signals at 1300 µm. Profile (d) from spot 4 shows no anoxic zone anymore. (**C**). Model of the oxygen distribution in the snottite biofilm. Indicated are the outer oxic part and the inner anoxic part.

(Stookey, 1970; Ziegler *et al.*, 2009). Sulfate quantification was conducted as described by Kolmert *et al.* (2000).

S and Fe K edge XANES spectroscopy. Microtome slices of the embedded biofilm that were also used for the microsensor analysis between spots 1 and 2 of the oxygen measurements (Figure 1A) were fixed on a Kapton tape. S and Fe *K* XANES spectra have been recorded at different sample positions across the biofilm. Measurements were done at the X-ray beamline of the synchrotron radiation laboratory for environmental studies (SUL-X) of the synchrotron radiation facility ANKA (Karlsruhe Institute of Technology, Karlsruhe, Germany) with a wiggler as radiation source.

Cryo-SEM. Scanning electron microscope (SEM) images were taken with a Zeiss Ultra Plus SEM (Zeiss, Oberkochen, Germany) equipped with a thermal Schottky field emitter (Zeiss). Snottite samples were clamped on a sample holder, frozen by plunging them into liquid nitrogen and transferred to the cryochamber (Alto 2500, Gatan, Munich, Germany). Here, surface water was removed by sublimation at $-95\,^{\circ}C$ before the sample was sputtered with Pt and introduced to the microscope.

Archaea enrichment. Parts from snottite biofilms were inoculated in Hungate tubes containing a previously described anoxic medium (Huber and Stetter, 2001) to which 0.1% casein and 20 mM $Fe_2(SO_4)_3$ were added. The head space of the tubes was flushed with an 80% CO_2/20% H_2 gas mixture. Bacterial growth was inhibited by the addition of $2\,\mu g\,ml^{-1}$ vancomycin, $150\,\mu g\,ml^{-1}$ streptomycin, $50\,\mu g\,ml^{-1}$ kanamycin and $30\,\mu g\,ml^{-1}$ chloramphenicol.

Results

Characterization of the possible niches in the biofilm

Oxygen concentrations. Oxygen is a major parameter for niche formation. If oxygen is available, it will be used as primary electron acceptor even if some examples of simultaneous reduction of other electron acceptors are known (Johnson and McGinness, 1991). Due to this accentuated role, the oxygen concentration throughout the biofilm matrix was determined first. Oxygen measurements were conducted *in situ* using intact snottites that were still attached to the mine ceiling. Thus, dehydration or deformations were prevented since the continuous water flow through the matrix was not interrupted and the shape of the biofilm maintained. Horizontal profiles were recorded along the longitudinal axes of the snottites to detect the spatial variations of O_2 concentration as a function of depth or the proximity to the pyrite-rich ceiling (Figure 1A). Oxygen measurements were conducted on four different snottites and all showed large anoxic parts inside of sections 1, 2 and 3 of the biofilm. Oxygen concentrations declined rapidly from the outer to the inner part of the biofilm. The oxic zone at section 1 of the biofilm ended already after 700 µm, indicating a high respiration rate (Figure 1Ba). The oxic part slightly broadened at the profiles 2 and 3. Here, the snottite is thinner and the concentration of reduced electron donors might

be lower due to consumption in areas that are more closely localized to the ceiling (Figures 1Bb and Bc). In section 4 of the snottite, oxygen was detectable throughout the biofilm (Figure 1Bd). Here, the biofilm thickness is about 1800 μm, and the respiratory consumption due to electron donor limitation might not be sufficient to result in an anoxic zone, which would explain oxygen detection even in the biofilm center. In summary, partial areas of the biofilm are anoxic or contain oxygen concentrations below the detection limit of 1 p.p.b. (Figure 1C).

pH values. Similar to oxygen, pH profiles were also recorded at different positions of the biofilm using a micro-pH-electrode. In contrast to the variations seen with oxygen concentrations, the observed pH values were quite constant and varied only slightly around 2.05 (Figure 2). Hence, the influence of pH on the distribution of microbial species is most probably not as pronounced as the influence from oxygen. pH measurements were conducted several times in four different snottites and never showed variations above the level shown in Figure 2.

Elemental composition. Cryo-LA-ICP-MS from frozen cross sections was conducted to analyze spatial variations of selected elements throughout the biofilm. These variations could be due to a biologically induced secondary mineral formation or the simple capture of cationic species by the negatively charged microbial surface. The intensities of some measured isotopes were too low to differ substantially from the chamber background level. Concentrations of S, Fe, K, Na and Ni were above the detection limit but showed a rather constant distribution across the snottite (data not shown). To verify whether a difference in the concentration of dissolved elements between anoxic and oxic parts of the biofilm might exist, element concentrations were determined by ICP-MS or -OES using liquid samples from the anoxic and oxic regions of the biofilm (Table 1). Most of the analyzed elements did not differ in their concentration between the oxic and anoxic part of the biofilm. Only Na and K concentrations differed by >10%. The concentration of dissolved Na is 1.6-fold higher at the anoxic center compared to the oxic area, while the K concentration in the anoxic part is only 0.7-fold of what was detected at the oxic part (Table 1). Considering the amount of dissolved sulfur per liter (92–97 mM) as quantified by ICP-OES, it becomes evident that sulfate is the major contributor of the detected dissolved sulfur as the conducted sulfate quantifications from a whole biofilm via the method from Kolmert *et al.* (2000) reveal concentrations of 95 mM (±3.8 mM). The quantification of dissolved iron (47–50 mM) by ICP is in agreement with the quantifications of dissolved ferric (47.4±4.0 mM) and ferrous iron (8.3±1.5 mM) by the ferrozine assay (Stookey, 1970).

XANES spectra were recorded from cross sections to analyze species of the two major elements iron and sulfur throughout the biofilm (Supplementary Figure S1A). The Fe *K* XANES spectra across two slices differ in shape and edge positions (Supplementary Figure S1B andC). Via principal component analysis, only two iron species occurred over the whole biofilm. Although one species matches best with jarosite where Fe is trivalent, spectra with edges shifted to lower energies could not be identified directly (Supplementary Figures S1B and C). They represent either a Fe(II) species or a mixture of it with jarosite. The latter is assumed because the spectrum with the flank at the lowest energy of the series did not match with the ones of any known Fe(II) reference compound.

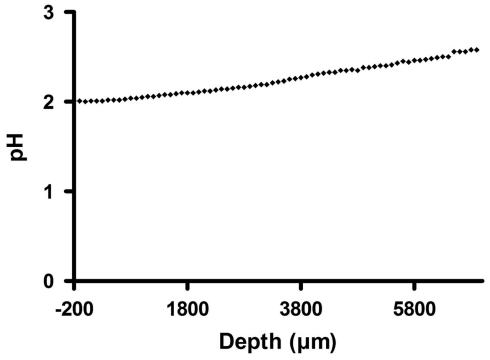

Figure 2 pH profile of a snottite. The data display a cross section as shown in Figure 1. at 1.5 cm distance from the pyrite ceiling. The pH ranges between 2 and 2.5 but there is no trend between biofilm rim and center.

Table 1 ICP MS/OES results

Sample	*Ca (OES) mg l⁻¹*	*Cu (MS) mg l⁻¹*	*Fe (OES) mg l⁻¹*	*K (OES) mg l⁻¹*	*Mn (OES) mg l⁻¹*
Biofilm anoxic part	393±1	210.5±0.4	2628±6	27.8±0.1	32.54±0.06
Biofilm oxic part	433.63±0.03	214±2	2807±5	39.73±0.01	34.79±0.07
Sample	*Na (OES) mg l⁻¹*	*Ni (MS) μg l⁻¹*	*P (OES) mg l⁻¹*	*S (OES) mg l⁻¹*	*V (MS) μg l⁻¹*
Biofilm anoxic part	251.8±0.3	527±7	8.8±0.2	2949±9	66.5±0.8
Biofilm oxic part	157.597±0.009	578±5	9.3±0.2	3125±9	61±0.5

Abbreviations: ICP, inductively coupled plasma; OES, optical emission spectrometry; MS, mass spectrometry.

A hypothetical end member spectrum—obtained by subtracting a jarosite spectral fraction until the white line or flank position of a typical Fe(II) spectrum is reached—shows spectral features similar to Fe(II) sulfate (Supplementary Figure S2). Hence, it is likely that the second Fe species originates from Fe(II), most likely dissolved in the aqueous phase or adsorbed on the organic constituents of the biofilm. The spectra that are closely related to jarosite could be measured in the oxic part of the biofilm but similar spectra were recorded also in the anoxic center (Supplementary Figure S1 B: locations 1, 22 and C: locations 2, 10 and 25). The S *K* XANES spectra are more complex than the Fe *K* edge spectra. Principal component analysis results in four to five components. Peak positions in the spectra are 2472.4, 2475.2, 2480.2 and 2481.5 eV (Supplementary Figure S3). The latter is in agreement with the positions known for sulfatic sulfur (S^{6+}). Especially at the oxic part of the slices, sulfate is the dominant species, which correlates with the identification Fe *K* XANES spectra from the oxic areas that have been identified as containing a major fraction of jarosite. In comparison with appropriate references, peak 2472.4 could be identified as thiol group R-S-H and peak 2475.2 as a sulfoxide R-(S=O)-R. Peak 2480.2 is related to RSO_3 units, here represented by anthraquinone-2-sulfonic-acid, which is only found in the anoxic part (Supplementary Figure S4).

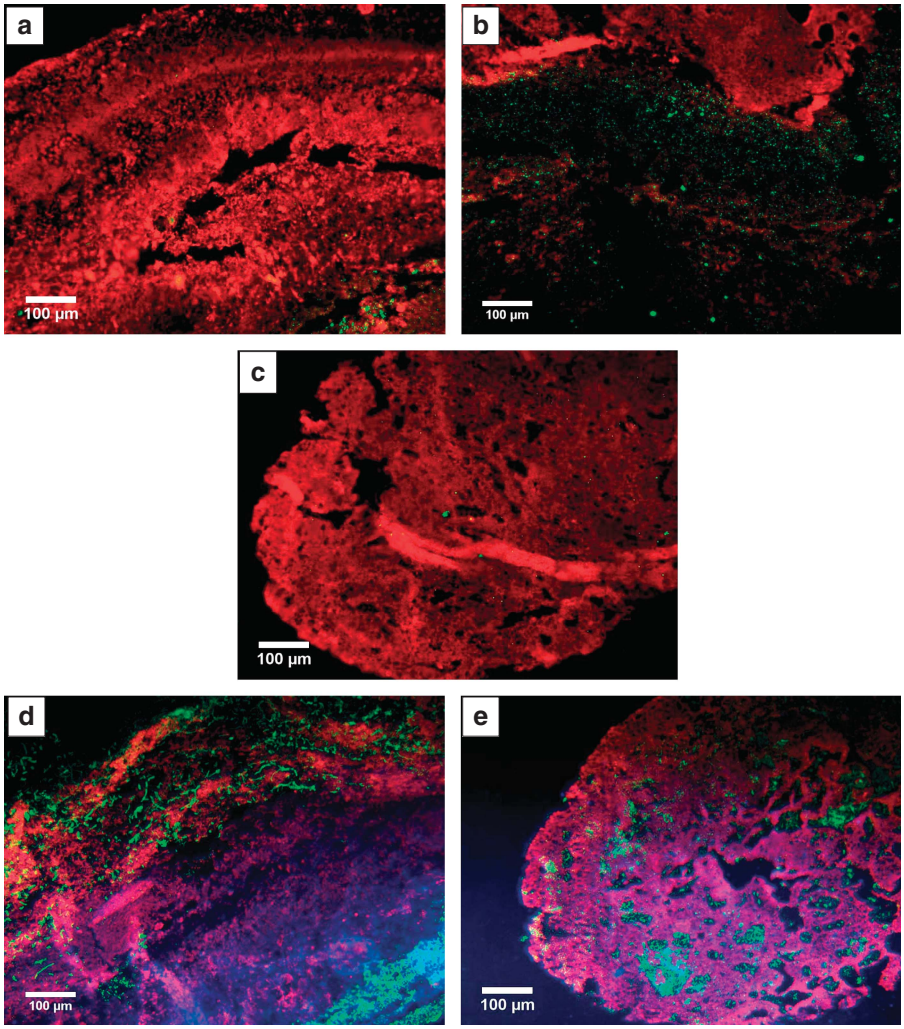

Figure 3 CARD FISH pictures of a cross section of the snottite. (**a**) In the upper part (Spot 1, Figure 1A) of the snottite bacteria (EUB338, Alexa 546 in red) can be seen throughout the whole cross section while the archaeal signal (ARCH915, Alexa 488 in green) is only in the middle part, which is most likely fully anoxic. (**b**) Inner area of the upper part of the biofilm (Spot 1, Figure 1A). Archaea (ARCH915, Alexa 488 in green) are found in high abundance. (**c**) Bacteria (EUB338, Alexa 546 in red) and archaea (ARCH915, Alexa 488 in green) in the lower part of the biofilm (Spot 4, Figure 1A). The image shows that the whole biofilm is populated by bacteria but almost no archaea-derived signal is detectable. (**d**) Image of the upper part (Spot 1, Figure 1A) of the snottite. The *Acidithiobacillus* species (THIO1, Alex 488 in green) are in the very outer and in the inner part while we see *Leptospirillum ferrooxidans* (LEP636, Alexa 546 in red) in a broad outer area. DAPI (4,6-diamidino-2-phenylindole) in blue shows all cells. (**e**) In the lower part of the snottite (Spot 4, Figure 1A) where no anoxic zone was detectable (Spot 4, Figure 1A), an unspecific distribution of the *Leptospirillum* (LEP636, Alexa 546 in red) and *Acidithiobacillus* (THIO1, Alex 488 in green) species is found. DAPI stain shows all organisms in blue.

Microorganisms in the biofilm

First, hybridizations with general probes for bacteria (probe EUB 338, Supplementary Table S1) and archaea (probe ARCH915) were conducted. Cross sections from Figure 1A were analyzed by CARD FISH. At section 1 (Figure 1A), all detectable archaea inhabit the anoxic zone of the snottite and cannot be spotted in the oxic areas (Figures 3a and b). Correlating with this observation, the cross section from area 4 (Figure 1A) of the biofilm contains very few to almost no archaeal signals (Figure 3c). Thereafter, further identification of the microbial population was conducted using 454 pyro-sequencing of isolated snottite DNA from biofilms collected in the first level. Using this approach, 647 reads with 16S rRNA sequence information were able to be classified into a phylum. A total of 96.3% of these sequences (reads) could be attributed to the bacteria, while only 3.7% archaeal sequences were obtained. Within the bacterial sequences, about 74.1% could be ascribed to the genus *Leptospirillum*. As can be seen in Figure 4, the next most abundant organisms are species belonging to the genus *Acidithiobacillus* (10.5% of the bacterial community). These results are supported by the CARD FISH experiments. Using more specific bacterial probes, we found that the bacterial community consists mainly of *Acidithiobacillus* sp. (probe THIO1) and *L. ferrooxidans* (probe LEP636). The probes for *Leptospirillum* group II (probe LEP154) did not result in any signal while we found occasional signals from *Leptospirillum* group III (probe LEP634) (data not shown). *L. ferrooxidans* species inhabit a major part of the oxic part of the biofilm rim. Acidithiobacilli can be detected not only in the oxic but also in the anoxic part of the cross sections (Figures 3d and e). In summary, as shown by pyro-sequencing and CARD FISH experiments, the microbial population is mainly composed by bacteria, more precisely by *Leptospirillum* spp. and *Acidithiobacillus* spp. Interestingly, neither in the CARD FISH experiments nor in the sequencing data we could detect *Ferrovum* sp., which were found in former studies from the adit level of the mine (Ziegler *et al.*, 2009). In the metagenomic data also, other typical acidophilic bacteria were detected in minor abundance—mainly *Proteobacteria* and *Actinobacteria*—like the iron-reducing bacterium *Ferrimicrobium* sp. (Figure 4).

In former studies, no archaea were detected in biofilms of this mine (Ziegler *et al.*, 2009). Due to the low coverage of the archaeal sequences from the metagenome, we used restriction fragment length analysis and subsequent sequencing to gain a deeper understanding of the archaeal community. General archaea primers failed to amplify an archaeal 16S rRNA gene signal. By contrary, primers deduced

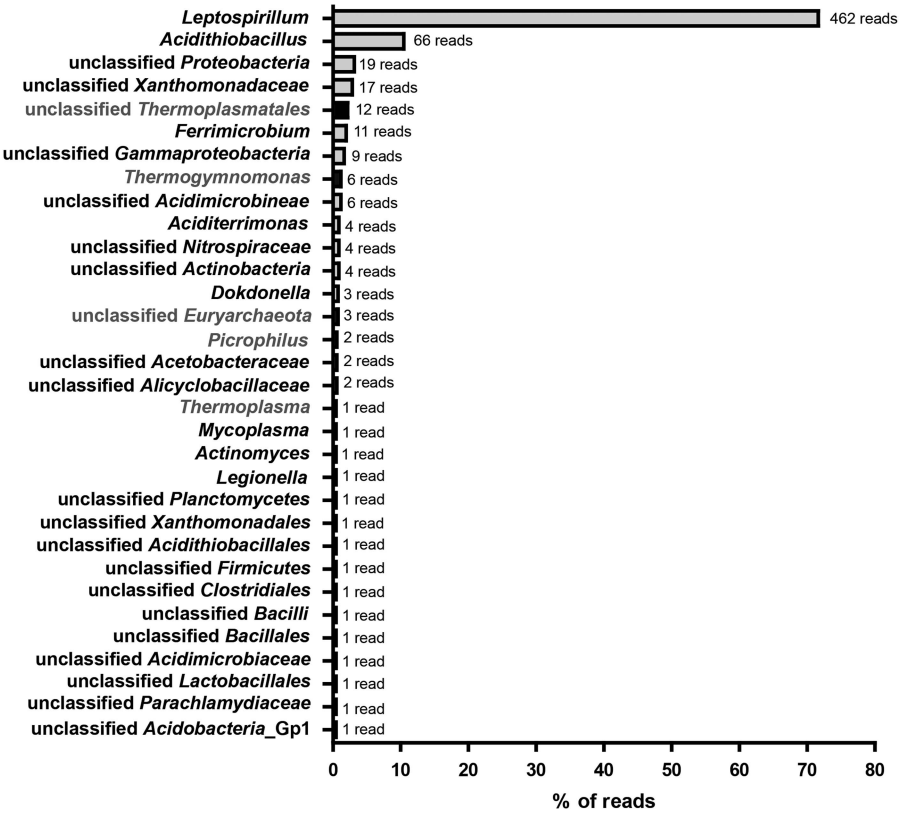

Figure 4 454 pyro-sequencing 16S rDNA results from the second level of the pyrite mine 'Drei Kronen und Ehrt'. Species classified by Ribosomal Database Project classification of the metagenome reads. The absolute number of reads is shown at the tip of the bar and the amount in percentage of all reads with 16S information is displayed along the x axis. *Leptospirillum* spp. builds the main population of the microorganism community. Acidithiobacilli are the next most abundant species.

from the archaeal probe ARCH915 combined with a universal primer and specific primers for the recently discovered ARMAN-enabled PCR product formation (Supplementary Table S2) (Baker *et al.*, 2006). Sequence analysis revealed the presence of clones most closely related to the ARMAN species described by Baker *et al.* (2006) as well as clones belonging to the *Thermoplasmatales*. The detected ARMAN clones (ARMAN-Clone_HM_4–46% abundant; ARMAN-Clone_HM_7–50% and ARMAN-Clone_HM_29–4%) cluster in the ARMAN branch together with other uncultured archaea clones from the Rio Tinto (Amaral-Zettler *et al.*, 2011). The *Thermoplasmatales* sequences are mainly related to a branch with uncultured representatives of this order, whereas one type (Archaea-Clone_HM_19–40% from all archaea clones) is related to *Ferroplasma* (Figure 5). The closest relatives to Archaea-Clone_HM_2 (42%), Archaea-Clone_HM_20 (6%) and Archaea-Clone_HM_21 (13%) are so far uncultured representatives from other acidic environments found in the Iberian Pyrite Belt (Figure 5) (Rowe *et al.*, 2007; Amaral-Zettler *et al.*, 2011; Gonzalez-Toril *et al.*, 2011). Based on the restriction fragment length polymorphism results, more specific probes for the detection of ARMAN and *Thermoplasmatales* were used. We see clearly the *Thermoplasmatales* signal correlating with the archaeal signal. *Thermoplasmatales* seem to represent the major group of archaea in the biofilm that is also corroborated by the 454 sequencing results (Figure 4 and Supplementary Figure S5A). The ARMAN signal does not clearly correspond to the general archaeal probe but is always located in the same area (Supplementary Figure S5B). In summary, archaea present in the biofilm are related to uncultured *Thermoplasmatales* and novel ARMAN species and prefer the anoxic part of the biofilm.

The described experiments identified the different niches within the biofilms and their microbial population. However, what was missing was a clear picture how this community might look under *in situ* conditions. Cryo-SEM was conducted to gain this information and the images display microorganisms embedded in a complex mixture of exopolysaccharide structures and secondary minerals (Figure 6). Jarosite crystals with their typical pseudocubic habitus dominate the secondary minerals.

Enrichment of ARMAN

It was surprising to see that microbes belonging to the recently described ARMAN group were found exclusively in the anoxic parts of the biofilm, as it was assumed before that they rather have an aerobic lifestyle (Baker *et al.*, 2010). To corroborate this

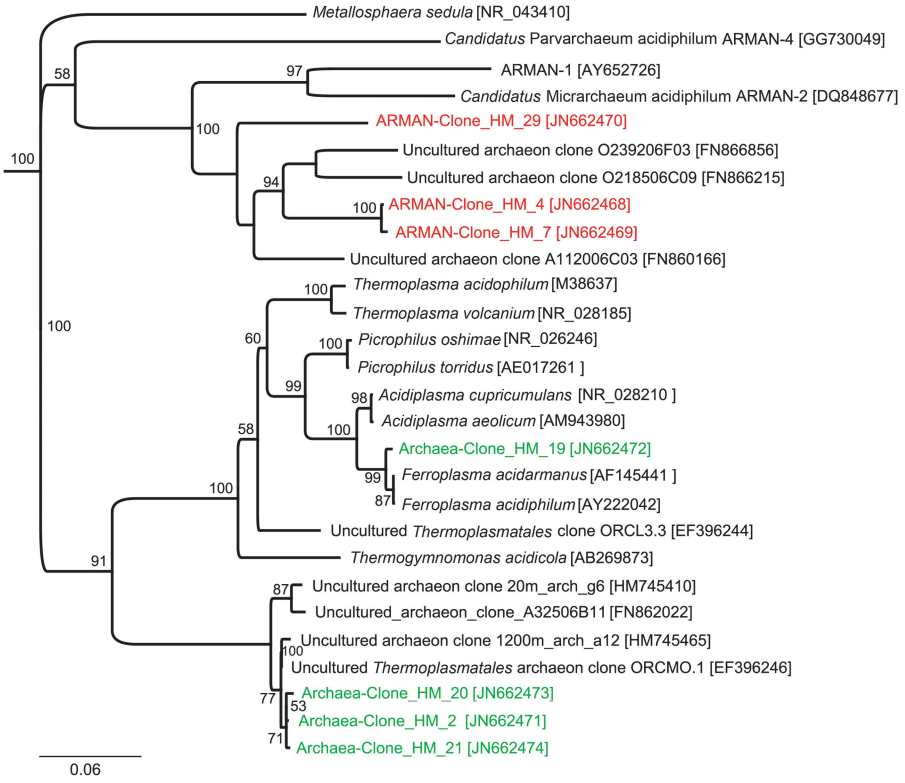

Figure 5 16S rDNA-based phylogenetic tree of the detected archaea and related sequences. Green indicates sequences from the archaeal primer pair (Supplementary Table S2, primers 1 + 2), red sequences gained from the ARMAN primers (Supplementary Table S2, primers 3 + 4). The neighbor-joining method was used and bootstrap was calculated from 1000 replicates. Bootstrap values >50 are indicated in the graph.

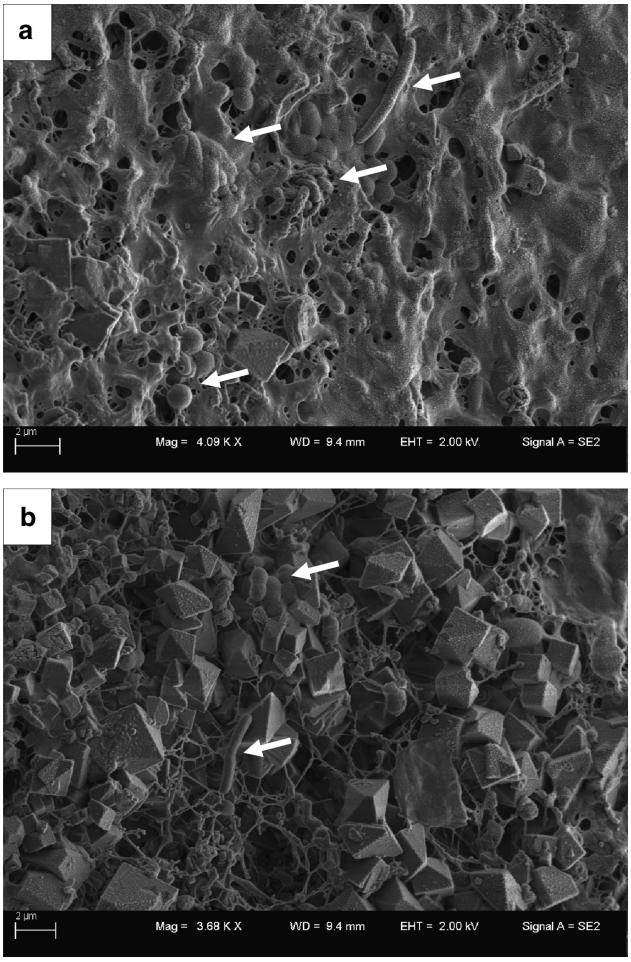

Figure 6 Cryo-SEM secondary electron images from the biofilm. (**a**) The image shows microorganisms and some jarosite crystals embedded in the matrix. Noticeable are rod like structures and cocci as well as some curved rods (indicated by arrows). (**b**) High amount of jarosite crystals in the matrix. In between there are rod like structures and also coccoid microorganisms (indicated by arrows).

finding, it was tried to enrich ARMAN from the biofilms using anoxic culturing techniques. A sample from the biofilm was inoculated in an anoxic medium containing casein and yeast extract as possible sources for heterotrophic growth. Ferric iron sulfate was added as electron acceptor. The medium was further supplemented with a mixture of antibiotics to hamper bacterial growth. Meanwhile, we were able to transfer the culture up to 12 times. Oxygen contaminations were excluded using periodic microsensor measurements. Figure 7 shows the results of the enrichment experiments. Bacteria could not be detected in the culture anymore. ARMAN were abundant in all the steps of the enrichment procedure. It was so far not possible to separate them from other organisms that were still present in the enrichment cultures. During the enrichment procedure, an attempt was made to exclude the addition of yeast extract or casein as well as ferric iron. Either yeast extract or casein have to be present in the medium, otherwise microbial growth cannot be detected. Furthermore, ferric iron is a necessary constituent of the medium.

Primary production

$^{14}CO_2$ labeling experiments were conducted to localize the uptake of atmospheric CO_2 in the biofilm. Furthermore, CARD FISH analyses were used to trace this activity back to microbial genera. These experiments were conducted *in situ*. The MAR FISH images show silver crystals in the rim of the snottite that are due to $^{14}CO_2$ incorporation by autotrophic organisms (Figure 8). Correlations with fluorescent images reveal the exclusive influence of the bacterial community in CO_2-based biomass production. Archaea (probe ARCH915) appear again only in the central part of the cross section and show no detectable sign of fixation of atmospheric $^{14}CO_2$ (Figures 8a and b). Of note, silver crystals should not be mistaken for secondary minerals in the center of the cross section. Mineral crystals shine very bright in different foci while the silver crystals stay dark (Figures 8b and c). Further analysis revealed that *Nitrospira* (probe NTR712) and *Acidithiobacillus* spp. (probe THIO1) are the main primary producers. The CARD FISH signals correlate with the MAR spots in the outer part (Figure 8c). The *Nitrospira* signal is derived from *Leptospirillum* spp. These organisms and the acidithiobacilli are known for their autotrophic lifestyle (Balashova *et al.*, 1973; Gale and Beck, 1967). Notably, fixation of atmospheric CO_2 is detectable only at the rim of the biofilm and ranges $\sim 30\,\mu m$ in the inner part. However, *Nitrospira* and *Acidithiobacillus* spp. inhabit an area that is by far larger than these $30\,\mu m$, which raises the question whether dissolved H_2CO_3 is the carbon source for *Leptospirillum* and *Acidithiobacillus* species that are localized to the inner part of the biofilm or whether the MAR FISH method was not sensitive enough to detect a probably lower rate of CO_2 fixation by these organisms.

Discussion

Microbial niches in the biofilm

The most surprising result of this study is the exclusive localization of archaea in anoxic areas of the consortium. Quantification of pH and the concentration of several elements did not point toward other factors contributing to niche formation. The detected archaeal sequences are related to the recently discovered ARMAN organisms as well as to uncultured *Thermoplasmatales* clones and organisms belonging to the genus *Ferroplasma*. Baker *et al.* (2010) proposed an aerobic lifestyle of ARMAN organisms based on metagenomic and proteomic data. This proposition is partly based on the abundance of a protein similar to succinate

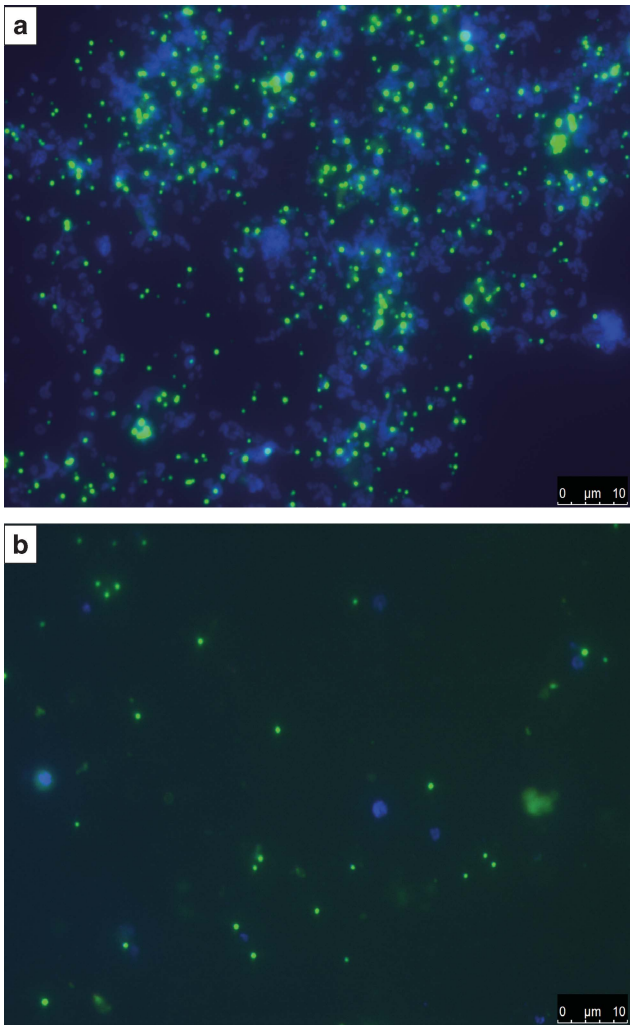

Figure 7 CARD FISH images of the ARMAN enrichment. (**a**) A culture that was transferred the eleventh time. The enrichment was growing for 9 weeks at the time of fixation. ARMAN can be seen in green (ARM980, Alexa 488) and DAPI ((4,6-diamidino-2-phenylindole); blue) stained all cells in the enrichment. (**b**) Culture transferred from (**a**) after 5 weeks of growth. Again ARMAN are in green (ARM980, Alexa 488) and DAPI in blue.

ubiquinone oxidoreductases in the protein pool. This enzyme is well known for its position within the citric acid cycle. The canonical enzyme catalyzes the oxidation of succinate to fumarate ($\grave{E}^{\circ} = 0 \pm 10$ mV) coupled to ubiquinone reduction (Clark, 1960). It is most probably the redox potential of this reaction and the often seen downregulation of the citric acid cycle under anoxic conditions that might have led to the assumption of an aerobic metabolism of the ARMAN detected at Iron Mountain. Nevertheless, succinate ubiquinone oxidoreductases and the anaerobic fumarate reductase cannot be distinguished easily. Furthermore, it was shown that succinate ubiquinone oxidoreductases can also function with menaquinone (Maklashina *et al.*, 1998). Moreover, the citric acid cycle can be an integral part of the central metabolism also for anaerobic organisms. The used carbon source would have to be known in order to make an assumption as to whether the tricarboxylic acid cycle fulfills only a function in building block production or furthermore in the generation of reducing equivalents for anaerobic respiration. Additionally, other genes, potentially involved in a respiratory chain to oxygen, were not detected (Baker *et al.*, 2010). The revealed occurrence of enzymes responding to oxidative stress like the superoxide dismutase do not necessarily have to indicate an aerobic lifestyle as the detoxification mechanisms operate also in strict anaerobes (Brioukhanov and Netrusov, 2004).

The *Ferroplasma*-related sequences detected in the biofilm show strong similarities to *F. acidiphilum* and '*F. acidarmanus*'. While *F. acidiphilum* is a strict aerobic autotroph (Golyshina *et al.*, 2000), '*F. acidarmanus*' is a facultative anaerobe that can respire anaerobically using ferric iron as an electron acceptor (Dopson *et al.*, 2004). Hence, organisms related to *Ferroplasma* could also inhabit an anoxic niche within the biofilm.

A number of the identified ribosomal rRNA gene sequences are similar to uncultured *Thermoplasmatales* and, from a phylogenetic point of view, only distantly related to the species isolated so far. The more related sequences from uncultured organisms stem from other acidic environments like the Iberian Pyrite Belt, including Rio Tinto (Rowe *et al.*, 2007; Amaral-Zettler *et al.*, 2011; Gonzalez-Toril *et al.*, 2011). Due to their remote position in the phylogenetic tree and as there is no isolated species belonging to these deeply branching organisms, it is not possible to assign certain physiological characteristics yet.

The main iron oxidizers in the studied bacterial consortium are *L. ferrooxidans* and *Acidithiobacillus*. They are also the most abundant microorganisms in the biofilm (Figures 3d and e and 4). As expected, organisms belonging to the genus *Leptospirillum* can be detected solely in oxic parts of the biofilm, which is certainly due to the fact that they can only respire on oxygen with ferrous iron as an electron donor (Hippe, 2000). Acidithiobacilli are found in the oxic as well as in the anoxic part. They can thrive aerobically and anaerobically using oxygen or ferric iron as electron acceptors (Pronk and Johnson, 1992). *Ferrovum* sp. is meanwhile a third candidate for playing a role in ferrous iron oxidation at acidic conditions (Hallberg, 2010). Brown *et al.* (2011) and Jones *et al.* (2011) proposed recently that pH and ferrous iron concentration could dictate whether *Ferrovum* or *Acidithiobacillus* might dominate a microbial consortium. Their assumption is corroborated by the results from this and a previous study from Ziegler *et al.* (2009). In the adit level of the mine, the snottite biofilms contained *Ferrovum* species rather than acidithiobacilli, while *Ferrovum* species were not detected in the first level. This difference may be caused by pH (2.6 in the upper horizon, 2.05 in the lower

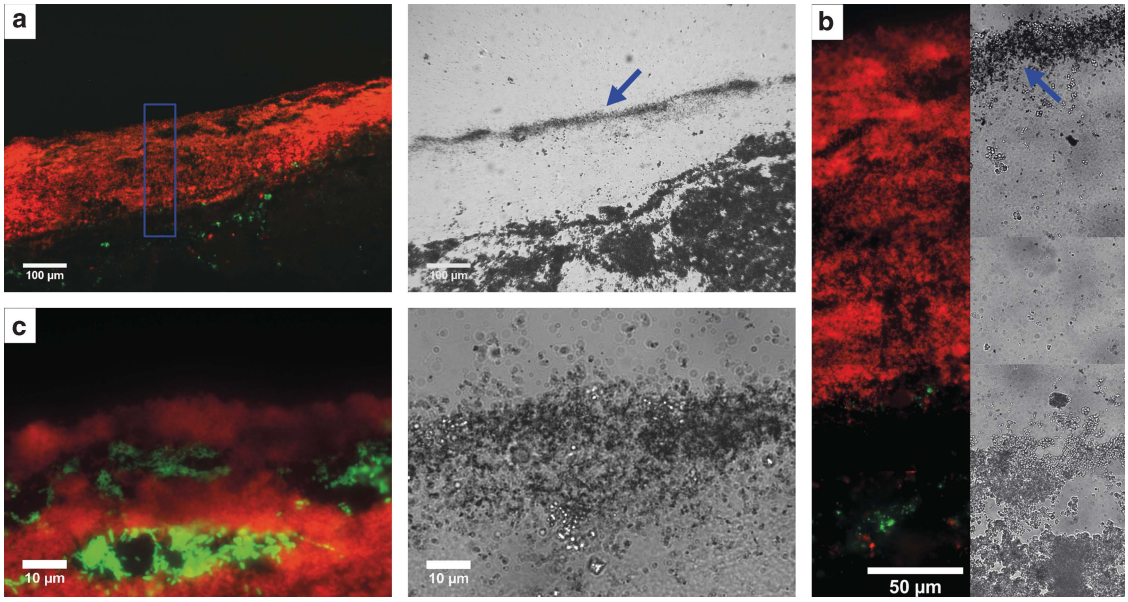

Figure 8 MAR FISH results from the ^{14}C labeled snottite. All cross sections are from the upper part of the biofilm (about 1–2 cm from the rock surface). Panels (**a**), (**b**) and (**c**) are arranged so that the biofilm surface can always be found at the top of the picture (**a**). Overview of a cross section showing bacteria (EUB338, Alexa 546 in red) and archaea (ARCH915, Alexa 488 in green). The archaea are again located in the middle of the snottite. The transmission picture correlates to the fluorescence image. Of note, silver crystals should not be mistaken for secondary minerals (mostly jarosite) that look similar on first sight but can be easily distinguished at higher magnification. The dark black fields in the upper part of the picture are mineralization and the small grayish dots in the middle show the MAR signal (indicated by an arrow). (**b**) Composite of five pictures illustrating the detail of Figure 8a (blue rectangle). Bacteria (EUB338, Alexa 546 in red) are localized throughout the sample while archaea (ARCH915, Alexa 488 in green) are only in the inner area. The transmission pictures show the MAR signals (indicated by an arrow). Mineral-derived signals are clearly distinct from the silver crystals. (**c**) *Nitrospira* (NTR 712, Alexa 546 red) and acidithiobacilli (THIO1, Alexa 488 in green) are in the outer part or the cross section. The transmission image shows the silver crystals formed due to the radioactive signals as dark black spots, while the light spots are minerals.

horizon) and/or Fe^{2+}concentration (15 mM in the upper horizon, 8.4 mM in the lower horizon) in the snottites. However, at both horizons of the mine, *L. ferrooxidans* dominates the consortia, and *Ferrovum*- or *Acidithiobacillus*-like organisms are companions rather than prevailing organisms.

The finding that archaea inhabit only the anoxic zone within a consortium of acidophiles was never shown before. Therefore this work gives new insights into the ecological niche of so far uncultured archaea belonging to *Thermoplasmatales* as well as to the ARMAN group first described by Baker *et al.* (2006). Based on the characterization of the habitat of the organisms, it was tried to enrich for ARMAN. It was possible to transfer the organisms several times in anoxic media, which corroborates the hypothesis of anaerobic growth of these organisms within the biofilm. Nevertheless, it was not possible so far to grow ARMAN in pure culture. These organisms might depend on catabolic end products of other organisms like the detected *Thermoplasmatales*.

Primary production and secondary consumption

Results from the conducted MAR FISH experiments suggest that primary production is mainly based on the CO_2-fixing activity of *L. ferrooxidans* and *Acidithiobacillus* species. Both are known chemolithoautotrophs (Maciag and Lundgren, 1964; Balashova *et al.*, 1973). There is a clear uptake of the $^{14}CO_2$ at the surface of the biofilm, but the signal disappears in a depth of about 30 µm inside. The signal loss can be either due to the detection limit of the MAR FISH technique or to the actual absence of active atmospheric CO_2 fixation deeper than 30 µm. Nevertheless, the center of the biofilm contains acidithiobacilli, which are—besides minor exceptions—obligate autotrophs. Hence, we have to assume that dissolved H_2CO_3 in the water that runs through the biofilm will be another carbon source for autotrophic growth. Furthermore, the activity of heterotrophic organisms could lead to CO_2 production and hence support autotrophic growth. This would imply that a complete carbon cycle is present in the biofilm.

Possible physiology of the uncultured archaea

The remaining question is what the physiological activity of archaea in the biofilm could be. The conducted oxygen sensor measurements suggest a facultative or strict anaerobic metabolism. Ferric iron or sulfate would be available as respiratory electron acceptors. The enrichments indicate a heterotrophic growth of the archaea. Organic carbon,

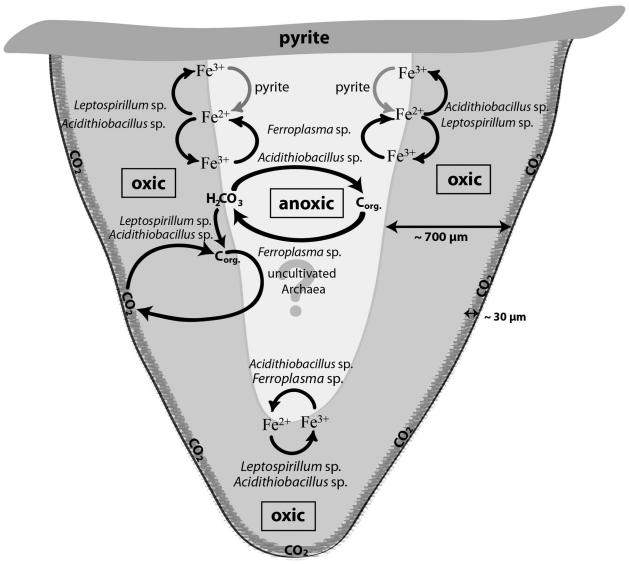

Figure 9 Model of possible carbon and iron fluxes in a snottite from the first level. The oxic (grey) and anoxic parts (white) are indicated. *Leptospirillum* species are solely found in the oxic part, whereas acidithiobacilli are found in the oxic as well as in the anoxic part. The archaea could only be detected in the anoxic zone. In the oxic area, ferrous iron oxidation can take place while in the anoxic part iron reduction by *Acidithiobacillus* sp. and *Ferroplasma* sp. is possible. Additionally, the iron can be reduced abiotically via pyrite dissolution (grey arrows). Atmospheric CO_2 fixation could only be detected in the surface area, approximately in the first 30 µm. Behind this point, a possible carbon source could be dissolved H_2CO_3. The inorganic carbon can be fixed by the primary producers like the autotrophic acidithiobacilli and leptospirilla. Heterotrophic organisms like *Ferroplasma* sp. can use the resulting organic carbon sources to sustain their energy and carbon metabolism. The role of the uncultivated archaea is so far not proven but heterotrophic growth is most likely.

for instance, in the form of sugars or peptides is available in the biofilm matrix and could serve as carbon and/or electron source for heterotrophic growth. A fermentative lifestyle of the occurring archaea would also certainly be possible. The conducted XANES experiments lead us to a further hypothesis. Sulfur in the form of a sulfonic acid as well as a thiol are present in the biofilm. There are only a few examples of naturally occurring sulfonic acids in the environment (White and Zhou, 1993). Adding the occurrence of a sulfonic acid and archaea together gives rise to the hypothesis that coenzyme M might have been identified via XANES analysis. Coenzyme M would be a very specific marker for the presence of methanogenic archaea, independent of whether they are hydrogenotrophic or acetoclastic (Elias *et al*., 1999). These hypotheses need to be proven in isolated cultures. A first step towards this was done by the archaea enrichment experiments.

The results of this study and the hypotheses gained from these results are summarized in a model in Figure 9. It seems obvious that a full carbon and iron cycle operates in the snottite biofilms. The consortium is based on primary production by *Acidthiobacillus* as well as *Leptospirillum* species. Archaea occur in lower abundance and only in the center of the biofilm. They seem to operate as secondary organisms, which grow using organic carbon provided by the primary producers. Ferric iron might be the respiratory electron acceptor. Fermentative growth using organic molecules of the biofilm matrix would also be possible.

Acknowledgements

We thank Professor Georg Fuchs for all the assistance, Professor Peter Graumann and Felix Dempwolff for access to the fluorescence microscopes. We gratefully acknowledge Dr Nicole Dubilier and Silke Wetzel from the MPI Bremen for sharing their FISH knowledge with us. Thanks to Dr Horst Scheffler and Gerd-Otto Herrmann from the pyrite mine 'Drei Kronen und Ehrt'. Thanks to Dr Andrea Wieland for assistance with the oxygen electrode. Thanks to A Voegelin for providing the Fe(II)sulfate spectrum, to Ralph Steininger (ANKA) for helpful discussions about PCA analysis and for beamtime at ANKA. Thanks to Florian Mann for help with the Metagenome data. SZ greatly appreciates the scholarship of the State Law on Graduate Funding Baden-Württemberg. This work was funded by the DFG, Grant no. GE2085/4-1.

References

Amaral-Zettler LA, Zettler ER, Theroux SM, Palacios C, Aguilera A, Amils R. (2011). Microbial community structure across the tree of life in the extreme Rio Tinto. *ISME J* **5**: 42–50.

Baker BJ, Comolli LR, Dick GJ, Hauser LJ, Hyatt D, Dill BD *et al.* (2010). Enigmatic, ultrasmall, uncultivated Archaea. *Proc Natl Acad Sci USA* **107**: 8806–8811.

Baker BJ, Tyson GW, Webb RI, Flanagan J, Hugenholtz P, Allen EE *et al.* (2006). Lineages of acidophilic archaea revealed by community genomic analysis. *Science* **314**: 1933–1935.

Balashova VV, Vedenina IY, Markosyan GE, Zavarzin GA. (1973). The auxotrophic growth of *Leptospirillum ferrooxidans*. *Mikrobiologiya* **43**: 581–585.

Bond PL, Druschel GK, Banfield JF. (2000). Comparison of acid mine drainage microbial communities in physically and geochemically distinct ecosystems. *Appl Environ Microbiol* **66**: 4962–4971.

Brioukhanov AL, Netrusov AI. (2004). Catalase and superoxide dismutase: distribution, properties, and physiological role in cells of strict anaerobes. *Biochemistry* **69**: 949–962.

Brown JF, Jones DS, Mills DB, Macalady JL, Burgos WD. (2011). Application of a depositional facies model to an acid mine drainage site. *Appl Environ Microbiol* **77**: 545–554.

Clark WM. (1960). *Oxidation-Reduction Potentials of Organic Systems*. Waverly Press: Baltimore, MD, USA.

Cole JR, Wang Q, Cardenas E, Fish J, Chai B, Farris RJ *et al.* (2009). The Ribosomal Database Project: improved alignments and new tools for rRNA analysis. *Nucleic Acids Res* **37**: D141–D145.

Dopson M, Baker-Austin C, Hind A, Bowman JP, Bond PL. (2004). Characterization of Ferroplasma isolates and *Ferroplasma acidarmanus* sp. nov., extreme

acidophiles from acid mine drainage and industrial bioleaching environments. *Appl Environ Microb* **70**: 2079–2088.

Elias DA, Krumholz LR, Tanner RS, Sulfita JM. (1999). Estimation of methanogen biomass by quantitation of coenzyme M. *Appl Environ Micobiol* **65**: 5541–5545.

Gale NL, Beck JV. (1967). Evidence for the calvin cycle and hexose monophosphate pathway in *Thiobacillus ferrooxidans*. *J Bacteriol* **94**: 1052–1059.

García-Moyano A, González-Toril E, Aguilera A, Amils R. (2007). Prokaryotic community composition and ecology of floating macroscopic filaments from an extreme acidic environment, Río Tinto (SW, Spain). *Syst Appl Microbiol* **30**: 601–614.

Golyshina OV, Pivovarova TA, Karavaiko GI, Kondrateva TF, Moore ER, Abraham WR *et al.* (2000). Ferroplasma acidiphilum gen. nov., sp. nov., an acidophilic, autotrophic, ferrous-iron-oxidizing, cell-wall-lacking, mesophilic member of the Ferroplasmaceae fam. nov., comprising a distinct lineage of the Archaea. *Int J Syst Evol Microbiol* **50**(Pt 3): 997–1006.

Gonzalez-Toril E, Aguilera A, Souza-Egipsy V, Lopez Pamo E, Sanchez Espana J, Amils R. (2011). Geomicrobiology of La Zarza-Perrunal acid mine effluent (Iberian Pyritic Belt, Spain). *Appl Environ Microbiol* **77**: 2685–2694.

Hallberg KB. (2010). New perspectives in acid mine drainage microbiology. *Hydrometallurgy* **104**: 448–453.

Hallberg KB, Coupland K, Kimura S, Johnson DB. (2006). Macroscopic streamer growths in acidic, metal-rich mine waters in north wales consist of novel and remarkably simple bacterial communities. *Appl Environ Microbiol* **72**: 2022–2030.

Hippe H. (2000). Leptospirillum gen. nov. (ex Markosyan 1972), nom. rev., including *Leptospirillum ferrooxidans* sp. nov. (ex Markosyan 1972), nom. rev. and *Leptospirillum thermoferrooxidans* sp. nov. (Golovacheva et al. 1992). *Int J Syst Evol Microbiol* **50**(Pt 2): 501–503.

Huber R, Stetter KO. (2001). Thermoplasmatales. In: *The Prokaryotes: An Evolving Electronic Resource for the Microbiological Community: Dworkin M, Falkow S, Rosenberg E, Schleifer K-H, Stackebrandt E (eds) Springer: New York, NY, USA.*

Johnson DB, Hallberg KB. (2005). Acid mine drainage remediation options: a review. *Sci Total Environ* **338**: 3–14.

Johnson DB, McGinness S. (1991). Ferric iron reduction by acidophilic heterotrophic bacteria. *Appl Environ Microbiol* **57**: 207–211.

Jones D, Brown J, Larson L, Mills D, Burgos W, Macalady J. (2011). Ecological niches of Fe-oxidizing acidophiles in a coal mine discharge. In Goldschmidt Abstracts 2011. *Mineral Mag* **75**: 1092–1131.

Kimura S, Bryan CG, Hallberg KB, Johnson DB. (2011). Biodiversity and geochemistry of an extremely acidic, low-temperature subterranean environment sustained by chemolithotrophy. *Environ Microbiol* **13**: 2092–2104.

Kolmert A, Wikstrom P, Hallberg KB. (2000). A fast and simple turbidimetric method for the determination of sulfate in sulfate-reducing bacterial cultures. *J Microbiol Methods* **41**: 179–184.

Kriews M, Dunker E, Reinhardt H, Beninga I, Hoffmann E, Lüdtke C. (2001). *Patentschrift* DE000019934561C2.

Kriews M, Reinhardt H, Dunker E, Beninga I, Ruhe W. (2004). *Utility Patent* DE 20 2004 005 9916.

Lo I, Denef VJ, VerBerkmoes NC, Shah MB, Goltsman D, DiBartolo G *et al.* (2007). Strain-resolved community proteomics reveals recombining genomes of acidophilic bacteria. *Nature* **446**: 537–541.

Maciag WJ, Lundgren DG. (1964). Carbon dioxide fixation in the chemoautotroph, Ferrobacillus ferrooxidans. *Biochem Biophys Res Commun* **17**: 603–607.

Maklashina E, Berthold DA, Cecchini G. (1998). Anaerobic expression of *Escherichia coli* succinate dehydrogenase: functional replacement of fumarate reductase in the respiratory chain during anaerobic growth. *J Bacteriol* **180**: 5989–5996.

Nordstrom DK. (2000). Advances in the hydrogeochemistry and microbiology of Acid Mine Waters. *Int Geol Rev* **42**: 499–515.

Okabe S, Kindaichi T, Ito T. (2004). MAR-FISH - An ecophisiological approach to link phylogenetic affiliation and in situ metabolic activity of microorganisms at a single-cell resolution. *Microb Environ* **19**: 83–98.

Pernthaler A, Pernthaler J, Amann R. (2004). Sensitive multi-color fluorescence in situ hybridisation for the identification of environmental microorganisms. *Mol Microb Ecol Man Second Ed* **3**: 711–726.

Pronk JT, Johnson DB. (1992). Oxidation and reduction of iron by acidophilic Bacteria. *Geomicrobiol J* **10**: 153–171.

Reinhardt H, Kriews M, Miller H, Schrems O, Ludke C, Hoffmann E *et al.* (2001). Laser ablation inductively coupled plasma mass spectrometry: a new tool for trace element analysis in ice cores. *Fresenius J Anal Chem* **370**: 629–636.

Rogers AW. (1979). *Techniques of Autoradiography*. Elsevier: New York, NY, USA.

Rowe OF, Sanchez-Espana J, Hallberg KB, Johnson DB. (2007). Microbial communities and geochemical dynamics in an extremely acidic, metal-rich stream at an abandoned sulfide mine (Huelva, Spain) underpinned by two functional primary production systems. *Environ Microbiol* **9**: 1761–1771.

Singer PC, Stumm W. (1970). Acidic mine drainage: the rate-determining step. *Science* **167**: 1121–1123.

Steedman HF. (1957). Polyester wax; a new ribboning embedding medium for histology. *Nature* **179**: 1345.

Stookey LL. (1970). Ferrozine—a new spectrophotometric reagent for iron. *Anal Chem* **42**: 779–781.

White RH, Zhou D. (1993). Biosynthesis of conenzymes in methanogens. In: Methanogenesis GJ*Ferry* (ed) Chapman and Hall: New York, NY, USA.

Zakrzewski M, Bekel T, Ander C, Pühler A, Rupp O, Stoye J *et al.* (2012). MetaSAMS—A novel software platform for taxonomic classification, functional annotation and comparative analysis of metagenome datasets. *J Biotechnol;* e-pub ahead of print 29 September 2012; doi: 10.1016/j.jbiotec.2012.09.013.

Ziegler S, Ackermann S, Majzlan J, Gescher J. (2009). Matrix composition and community structure analysis of a novel bacterial pyrite leaching community. *Environ Microbiol* **11**: 2329–2338.

Zielinski FU, Pernthaler A, Duperron S, Raggi L, Giere O, Borowski C *et al.* (2009). Widespread occurrence of an intranuclear bacterial parasite in vent and seep bathymodiolin mussels. *Environ Microbiol* **11**: 1150–1167.

Supplementary Information accompanies this paper on The ISME Journal website (http://www.nature.com/ismej)